ELSEVIER

Applied Acoustics 61 (2000) 173–182

applied acoustics

www.elsevier.com/locate/apacoust

Effects of compression on the sound absorption of fibrous materials

Bernard Castagnède [a,*], Achour Aknine [a], Bruno Brouard [a], Viggo Tarnow [b]

[a] *LAUM (UMR CNRS 6613), 72085 Le Mans Cedex 9, France*
[b] *AKP/DTU, Bygning 358, 2800 Lyngby, Denmark*

Received 17 September 1999; received in revised form 5 January 2000; accepted 21 January 2000

Abstract

During the compression of a fibrous mat, it is well known that the absorption properties are decreasing. In order to predict this change, some heuristic formulae are proposed which take into account the modifications of the physical parameters (porosity, resistivity, tortuosity and shape factors) which enter the standard "equivalent fluid" model. Numerical predictions are then discussed and compared to experimental data obtained on a fibrous material (uncompressed and then compressed) used in the automotive industry.

1. Position of the problem

There is an often asked question related to the engineering of the acoustical properties of porous media, which is to predict their evolution versus the state of mechanical compression of the fibrous mat. One should point out that during such compression, the various fibres are brought nearer from each others, while they do not experience any deformation, i.e. their radius a remains unchanged. For instance, in the field of automotive acoustics, the seat padding, is subjected under the passengers weight to some compression/expansion cycles which end by squeezing down the porous materials (fibrous or cellular). For a given homogeneous porous layer, such compression is followed by a decrease in terms of porosity as well as the same trend on the characteristic lengths, and in the same time by an increase of tortuosity and resistivity. The basic idea of the present work is to quantify these variations for a uniaxial (1D) and a surface-like (2D) compression sollicitation, and to determine

* Corresponding author. Tel.: +33-2-4383-3270; fax: +33-2-4383-3520.
E-mail address: bernard.castagnede@univ-lemans.fr (B. Castagnède).

0003-682X/00/$ - see front matter
PII: S0003-682X(00)00003-7

the influence of such variations on those of the acoustical impedances and absorption coefficient. In Section 2, one introduces the standard Johnson–Allard "equivalent fluid" model which is used in this work, then Section 3 is devoted to the study of the variations of the physical parameters versus the compression rate (as noted by n). Next, Section 4 discusses some numerical predictions, and quantitative trends. Finally, Section 5 provides some experimental results during a compression test which clearly demonstrates that the computations and numerical predictions are basically correct (at least for a moderate compression rate, in the range of 2).

2. Johnson–Allard "equivalent fluid" model

The general expressions for the effective fluid density $\rho(\omega)$ and the effective compressibility modulus of the fluid $K(\omega)$ are given in the research monograph Allard ([1], p. 92) written a few years ago:

$$\rho(\omega) = \alpha_\infty \rho_0 \left[1 + \frac{\sigma\phi}{j\omega\rho_0\alpha_\infty} G_J(\omega) \right] \tag{1}$$

$$K(\omega) = \gamma P_0 / \left[\gamma - (\gamma - 1) \left\{ 1 + \frac{\sigma'\phi}{jB^2\omega\rho_0\alpha_\infty} G'_J(B^2\omega) \right\}^{-1} \right] \tag{2}$$

where

$$G_J(\omega) \sqrt{\left(1 + \frac{4j\alpha_\infty^2 \eta\rho_0\omega}{\sigma^2\Lambda^2\phi^2} \right)} \tag{3}$$

and

$$G'_J(B^2\omega) = \sqrt{\left(1 + \frac{4j\alpha_\infty^2 \eta\rho_0\omega B^2}{\sigma'^2\Lambda'^2\phi^2} \right)} \tag{4}$$

with

$$\sigma' = \frac{8\alpha_\infty \eta}{\phi\Lambda'^2} \tag{5}$$

In such expressions, γ represents the adiabaticity constant (ratio of the specific heat at constant pressure onto the same quantity at fixed volume), P_0 the ambient pressure, B the Prandtl number, ϕ the porosity, α_∞ the tortuosity, $\omega = 2\,\pi f$ the angular frequency, σ the resistivity, ρ_o the density of the fluid at rest η, the air viscosity, Λ and Λ' the viscous and thermal characteristic lengths (also called shape

factors) [2,3]. The complex "sound wavespeed" inside the porous medium is then provided by the classical relationship, $c(\omega)=[K(\omega)/\rho(\omega)]^{1/2}$. The high frequency asymptotic limit of that equation, which is very useful for low frequency ultrasonic applications, is described elsewhere [4,5]. The characteristic acoustical impedance is then defined by its usual form: $Z(\omega)=[K(\omega)\rho(\omega)]^{1/2}$ The reflection coefficient at normal incidence R can be easily deducted from the non-dimensional normalized acoustical impedance $z(\omega)$:

$$R(\omega)=\frac{z(\omega)-1}{z(\omega)+1} \tag{6}$$

The absorption coefficient $A(\omega)$ is related to the reflection coefficient $R(\omega)$ as follows:

$$A(\omega)=1-\left|R(\omega)\right|^2 \tag{7}$$

This last equation is often used in terms of practical applications. This quantity is directly linked, through the various constitutive equations written above, to the five physical parameters (porosity, resistivity, tortuosity, and the two shape factors) of the standard Johnson–Allard "equivalent fluid" model.

3. Variations of the physical parameters versus the compression rate

One can ask the question of predicting the changes in terms of the five physical parameters occuring during a 1D compression of a fibrous mat. The general and rigorous answer to such question is not trivial for the parameters (tortuosity, resistivity, viscous characteristic length, cf. their definition below) which include in their definition some quantities related to fluid mechanics (mainly the microscopic fluid velocities). On the other hand, such dependance is eventually much easier to predict for the "geometrical" parameters [porosity, thermal characteristic length, as given by Eq (8)]:

$$\phi=\frac{V_{\text{air}}}{V_{\text{total}}};\qquad \sigma=\frac{S\Delta p}{hQ_{\text{v}}};\qquad \alpha_\infty=\frac{\dfrac{1}{V}\displaystyle\int_{\text{V}}u^2\,\mathrm{d}V}{\left(\dfrac{1}{V}\displaystyle\int_{\text{v}}u\,\mathrm{d}V\right)^2};\qquad \Lambda=2\frac{\int_{\text{v}}u^2\,\mathrm{d}V}{\int_{\text{s}}u^2\,\mathrm{d}S};$$
$$\Lambda'=2\frac{\int_{\text{v}}\mathrm{d}V}{\int_{\text{s}}\mathrm{d}S}=2\frac{V}{S}. \tag{8}$$

In these expressions, the volume and surface integrals are calculated over an "average" pore inside an homogeneization domain having a volume V. The microscopic velocity of the air particles is noted by u, while Δp represents a pressure difference between both sides of a porous layer having a thickness h, for which a Q_{V} air flow circulates through the surface S. Some tortuosity measurements have been performed on compressed and uncompressed fibrous mats and are collected in Table 1

Table 1

Sample	Uncompressed sample		Compressed sample	
	α_∞	$\Lambda(\times 10^{-4}\ \mathrm{m})$	α_∞	$\Lambda(\times 10^{-4}\ \mathrm{m})$
Material 1	1.0226	2.610	1.0409	0.949
Material 2	1.0134	2.014	1.0370	0.941
Material 3	1.0088	0.948	1.0154	0.427
Material 4	1.0263	0.973	1.0615	0.446

below. The compression was done by using a special sample holder with a two grid (one coarse and one finer) system on each side enabling to decrease the thickness of the fibrous material (1D compression), with a ratio $n = h_0/h$, fixed to an arbitrary value ($n = 2$). These measurements done with ultrasonic techniques did show that the tortuosity slightly increases, following a simple law of variation, as noted in Eq. (9). In fact, the part over one of tortuosity is simply multiplied by the compression rate factor.

$$\alpha_\infty^{(n)} = 1 - n(1 - \alpha_\infty^{(0)}) \tag{9}$$

This relation is difficult to rigorously demonstrate. By contrast, an analogous equation exists for the porosity, that could easily be derived by some simple calculations.

$$\phi^{(n)} = 1 - n(1 - \phi^{(0)}) \tag{10}$$

Moreover, one could also derive the following relationships for the characteristic lengths and the resistivity (cf. Appendix for further details):

$$\Lambda'_{(n)} = \frac{\Lambda'_{(0)}}{\sqrt{n}} + \frac{a}{2}\left(\frac{1}{\sqrt{n}} - 1\right); \quad \Lambda_{(n)} = \frac{\Lambda_{(0)}}{\sqrt{n}} + \frac{a}{2}\left(\frac{1}{\sqrt{n}} - 1\right); \quad \sigma_{(n)} = n\sigma_{(0)}, \tag{11}$$

where a represents the mean fibre diameter. The result for the thermal characteristic length Λ' can be approximately derived (cf. Appendix) for some simplified geometrical configurations and distributions of the fibres. The formulae dealing with the resistivity σ is obtained from the result of the 2D compression for which there exist a few theoretical calculations made by Tarnow [6–8]. In the case of a 2D compression, the above results can be generalized and one obtains the following equations (cf. Appendix for detailed calculations and further explanations):

$$\alpha_\infty^{(n)} = 1 - n^2\left(1 - \alpha_\infty^{(0)}\right); \quad \phi^{(n)} = 1 - n^2\left(1 - \phi^{(0)}\right), \tag{12}$$

$$\Lambda'_{(n)} = \frac{\Lambda'_{(0)}}{n} + a\left(\frac{1}{n} - 1\right); \quad \Lambda_{(n)} = \frac{\Lambda_{(0)}}{n} + a\left(\frac{1}{n} - 1\right); \quad \sigma_{(n)} = n^2\sigma_{(0)} \tag{13}$$

4. Numerical predictions for the absorption coefficient

Some numerical predictions have been run in order to illustrate the above developments. In these simulations the thickness is varied but the global mass of the material is kept unchanged (cf. Fig. 1). This case exactly corresponds to the real use of materials which are simply compressed or expanded (when $n < 1$).

The initial fibrous material has been selected with the following properties : $\phi = 0.99$; $\sigma = 10\ 700$ N m^{-4} s; $\alpha_\infty = 1.03$; $\Lambda = 180$ μm ; $\Lambda' = 510$ μm. It is a material mainly used in the automotive industry made with polyester fibres by the company 3M. Its mass/unit area, is 220 g/m^2, and the fibres average diameter approximately is $a = 15$ μm.

The simulation related to that example (variable thickness and constant mass) is very illustrative. When the fibrous mat experiences a compression, the absorption coefficient has a strong decrease, which is somewhat due to a "thickness effect". Despite the variations of the physical parameters which are all in the right direction (increase of the tortuosity and resistivity, decrease of the porosity and both characteristic lengths), it is mainly the drop in thickness which is responsible for the net diminution of

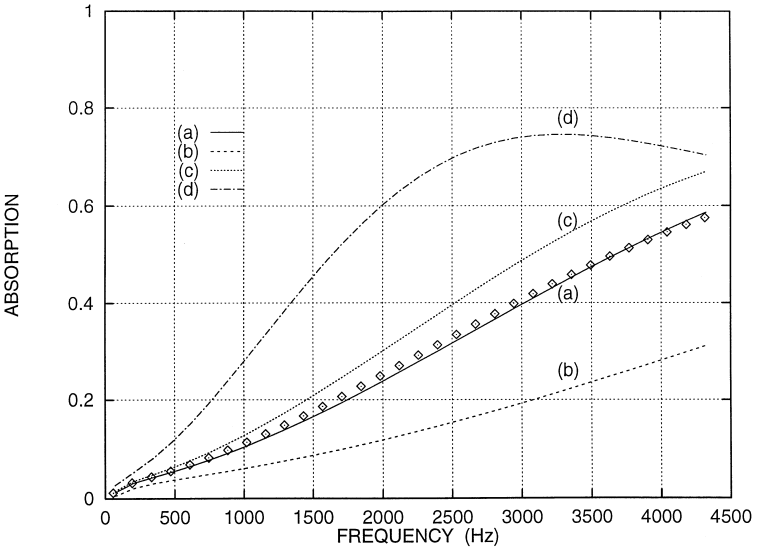

Fig. 1. Numerical simulations of the absorption coefficient as a function of frequency for a compressed fibrous material, (a) compression rate $n = 17/15 = 1.133$, as shown by continuous line (—). $\phi = 0.988$; $\sigma = 12\ 127$ N m^{-4} s; $\alpha_\infty = 1.034$; $\Lambda = 169$ μm; $\Lambda' = 479$ μm; (b) compression rate $n = 17/8.5 = 2$, as shown by dashed line (.....); $\phi = 0.98$; $\sigma = 21\ 400$ N m^{-4} s; $\alpha_\infty = 1.06$; $\Lambda = 127$ μm; $\Lambda' = 361$ μm; (c) compression rate $n = 17/18 = 0.944$, as shown by dots line (.....) $\phi = 0.991$; $\sigma = 10\ 106$ N m^{-4} s; $\alpha_\infty = 1.028$; $\Lambda = 185$ μm; $\Lambda' = 525$ μm; (d) compression rate $n = 17/34 = 0.5$, as shown by dashed-dot line (.....). $\phi = 0.995$; $\sigma = 5350$ N m^{-4} s; $\alpha_\infty = 1.015$; $\Lambda = 255$ μm; $\Lambda' = 721$ μm. The diamonds ($\diamond$) represent experimental data for $n = 17/15$. For each curve of Fig. 1, the ratio $n = h_0/h$, where h_o and h respectively represent the original thickness of the fibrous mat ($h_0 = 17$ mm), and h the value of that parameter for the compressed configuration. For Fig. 1 the reference values of the physical parameters are the following : $\phi = 0.99$; $\sigma = 10\ 700$ N m^{-4} s; $\alpha_\infty = 1.03$; $\Lambda = 180$ μm; $\Lambda' = 510$ μm.

the absorption coefficient. The opposite case of a 1D expansion of the fibrous material is followed by reversed trends, and a significant increase of the absorption coefficient. Again, this result is mainly due to a thickness effect which is prominent in front of the variations of the physical parameters being all in the wrong direction. One should notice that as close as $n = 0.5$, one observes a plateau in that improvement. Following these simulations, one can think about the concept of an optimum thickness for a given fibrous material, because of the significant changes of the absorption coefficient occuring on both sides of the nominal reference thickness.

5. Experimental validation and conclusions

A simple experimental validation has been done for a fibrous material, by measuring the coefficient of absorption with a research Kundt tube working with the TMTC (two microphones, three calibrations) method [9]. The measurements were performed on a similar material, characterized without compression, having physical parameters slightly different from those outlined in Section 4 (see caption of Fig. 2). Each of the five physical-parameters were independently measured without any fitting [10]. The comparison between the experimental data on the absorption coefficient and the corresponding predictions based on the Johnson–Allard "equivalent fluid" model (cf. Section 2) are presented in Fig. 2. The same fibrous material has also been tested with a nominal compression rate fixed to an arbitrary value $n = 50/31$. Fig. 3 shows the obtained results for that compressed configuration. For the

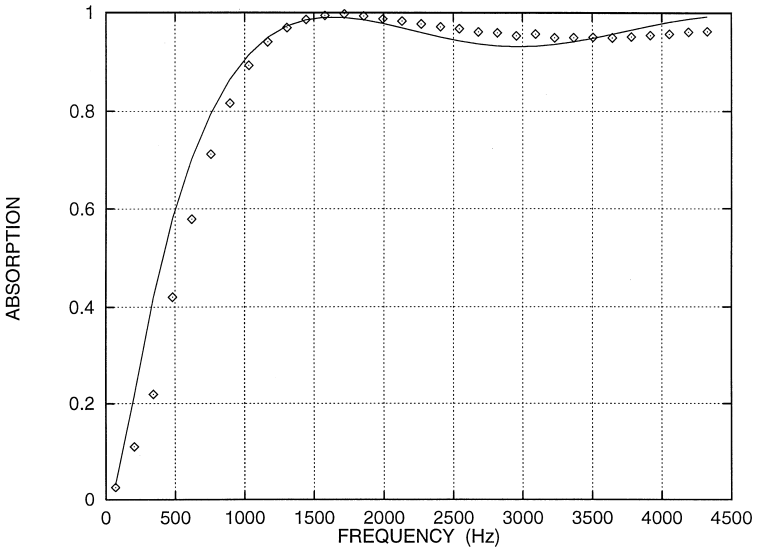

Fig. 2. Experimental data compared to numerical simulations of the absorption coefficient for an uncompressed fibrous material. The nominal thickness is $h_0 = 50$ mm and the physical parameters are the following: $\phi = 0.99$; $\sigma = 16\,950$ N m^{-4} s; $\alpha_\infty = 1.032$; $\Lambda = 107$ μm; $\Lambda' = 216$ μm. Experimental data: (◇), numerical predictions (—).

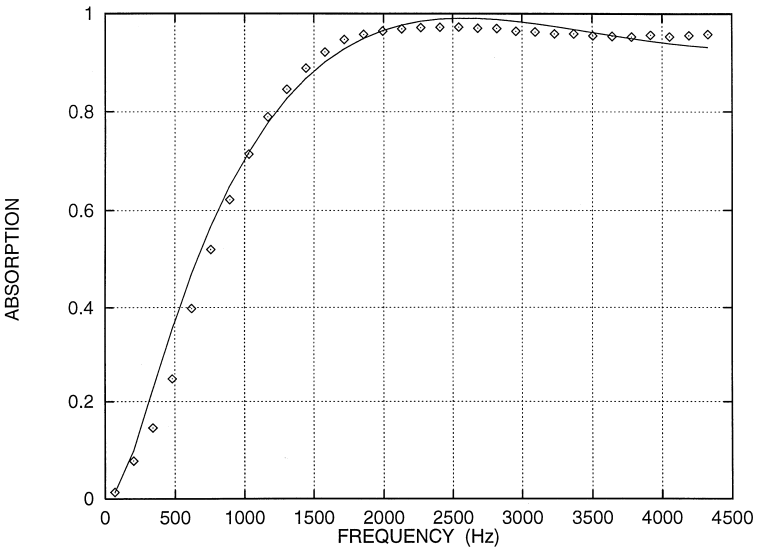

Fig. 3. Experimental data compared to numerical simulations of the absorption coefficient for a compressed fibrous material, with compression rate $n = 50/31 = 1.61$. The physical parameters are the following: $\phi = 0.984$; $\sigma = 27\ 339$ N m^{-4} s; $\alpha_\infty = 1.052$; $\Lambda = 84$ μm; $\Lambda' = 171$ μm. The reference values are given for the uncompressed configuration (i.e. Fig. 2). The compressed values of the physical parameters are computed according to Eqs. (9)–(11). Experimental data: (◇), numerical predictions (—).

modelling, we have used the transformation Eqs. (9)–(11) corresponding to a 1D compression. The results exhibit an excellent agreement between theoretical predictions and experimental data.

In this short report, some simple heuristic formulae have been proposed to take into account some changes occuring due to the compression of the fibrous network on the basic physical parameters describing the acoustical properties in terms of the standard "equivalent fluid" model. A 1D unidirectional compression is quite useful to describe the cramming down of fibrous materials occuring during their utilization. Some extra clues could also be deduced from a systematical use of simulation computer programs such as MAINE in order to model the influence of the microgeometry of the materials. These trends could also be efficiently used in order to optimize some preliminary design in terms of some peculiar applications.

Acknowledgements

Professor Jean-François Allard, who read a preliminary draft of that article, is gratefully acknowledged for detecting a few mistakes. We also wish to thank the EC NOCOMAT Thematic Network, BRRT-CT97-5024, for providing part of the financial support related to that work and authorizing the present publication. A special mention should also be given to the two reviewers who did an excellent expertise work, allowing us to significantly improve our contribution.

Appendix: Variations of some physical parameters during the compression of the pores

One consider the very simple geometrical configuration of a fibrous mat where the fibres are all infinite in length, uncurved and parallel, lying in the surface of the material. The incident acoustical field is normal to the material surface, i.e. it is orthogonal to the fibres. Besides porosity which is possible to evaluate during a 1-D compression, the thermal characteristic length is the most easy parameter to calculate, as it is simply twice the ratio of the average pore volume divided by its surface. The fibres are supposed not being affected by the compression (i.e. they do not experience any deformation during the compression of the material), and they keep their radius a unchanged. For the 2D compression case, one should imagine an uncompressed elementary fibre of radius a, surrounded by an "homogeneization" volume in the form of a concentric cylinder of radius b, having the same length L from those of the fibre. The calculation of Λ' provides:

$$\Lambda'_0 = \frac{2V}{S} = \frac{2L\pi\left(b^2 - a^2\right)}{2L\pi(b+a)} = b - a, \tag{A1}$$

and

$$\Lambda'_n = \frac{2L\pi\left(\frac{b^2}{n^2} - a^2\right)}{2L\pi\left(\frac{b}{n} + a\right)} = \frac{b}{n} - a = \frac{\Lambda'_0}{n} + a\left(\frac{1}{n} - 1\right). \tag{A2}$$

For the 1D compression case, calculations are less evident. One should instead use a "homogeneized" $b \times b$ square cell being compressed along one side, and similar calculations provide:

$$\Lambda'_0 = \frac{2V}{S} = \frac{2L\left(b^2 - a^2\right)}{4L(b+a)} = \frac{1}{2}(b-a) \tag{A3}$$

and

$$\Lambda'_n = \frac{2L\left(b\frac{b}{n} - a^2\right)}{2L\left(b + \frac{b}{n} + 2a\right)} = \frac{1}{2}\left[\frac{\left(\frac{b}{\sqrt{n}} - a\right)\left(\frac{b}{\sqrt{n}} + a\right)}{b\left(\frac{1+n}{2n}\right) + a}\right] \tag{A4}$$

In the case where the compression rate is close to one, $\frac{1+n}{2n} \approx \frac{1}{\sqrt{n}}$, and Eq. (A6) can be written down in the following approximate form:

$$\Lambda'_{(n)} = \frac{\Lambda'_{(0)}}{\sqrt{n}} + \frac{a}{2}\left(\frac{1}{\sqrt{n}} - 1\right) \tag{A5}$$

For most formulae, the first term is amply sufficient because $\Lambda' >> a$. For instance, for the materials described in this report a is approximately 15 μm.

The transformation relationship related to the viscous characteristic length should be very close because there generally exists a relation between both characteristic length (Λ and Λ'). For most fibrous materials, one observes $\Lambda' > \Lambda$, with $\Lambda'/\Lambda = 2$ or 3. For the sake of simplicity, one can then consider the same law of transformation for both characteristic lengths. Dealing with porosity, some elementary calculations could also be done which easily lead to Eqs. (10) and (12). Similar expressions for the tortuosity can also be derived for the 1D and 2D compression cases [cf. Eqs. (9) and (12)]. These predictive equations are also approximately verified by experimental data as emphasized in Section 2 (cf. Table 1). These expressions cannot be rigorously demonstrated, as the tortuosity contains in its definition the microscopic velocity of the fluid inside the pores, and accordingly there should be considered only as mere and crude approximations. Finally, for the resistivity σ, some predictions were made for several cases. For a granular material with spherical grains of radius r, it is well known that the resistivity is proportional to the inverse of its squared power r^2 [11]. For a fibrous mat, Tarnow did a few basic calculations to theoretically predict the resistivity [6,7]. These calculations show that for a regular array of infinite parallel uncurved fibres having a constant πa^2 section, the resistivity can be written [8] in the case of the flow being perpendicular to the fibres:

$$\sigma = \frac{2\pi\eta}{b^2\left[\ln\left(\frac{b}{a}\right) - 1.310\right]}, \tag{A6}$$

where b represents one side of the homogeneisation (in the form of a $b \times b \times h$ parallelepiped) and η the fluid viscosity. In fact, b is directly linked to the ratio of the density of the fibre ρ_g and to those of the fibrous mat ρ_w through the expression:

$$b = a\sqrt{\pi\frac{\rho_g}{\rho_w}} \tag{A7}$$

Because $\rho_g >> \rho_w$, this result being a direct consequence of the very high value of the porosity of the fibrous materials ($\phi > 0.96$), one verifies that $b >> a$, which allows some of the above approximations to be used. Moreover, the dependance on the resistivity which appears in Eq. (A6) as a function of $1/b^2$, is directly related to a 2D compressed configuration for which b^2 is divided by n^2, last result which confirms the relation $\sigma_{(n)} = n^2\sigma_{(0)}$. For a 1D compression, one can retrieve by a similar reasoning the qualitative dependance on the resistivity in the form $\sigma_{(n)} = n^2\sigma_{(0)}$.

References

[1] Allard JF. Propagation of sound in porous media: Modeling sound absorbing materials. London: Chapman and Hall, 1993.

[2] Lafarge D, Allard JF, Brouard B. Characteristic dimensions and predictions at high frequencies of the surface impedance of porous layers. J Acous Soc Am 1993;93:2474–8.

[3] Henry M, Lemarinier P, Allard JF. Evaluation of the characteristic dimensions for porous sound-absorbing materials. J Appl Phys 1995;77:17–20.
[4] Leclaire P, Kelders L, Lauriks W, Melon M, Brown NR, Castagnède B. Determination of the viscous and thermal characteristic lengths of plastic foams by ultrasonic measurements in helium and air. J Appl Phys 1996;80:2009–12.
[5] Castagnède B, Aknine A, Melon M, Depollier C. Ultrasonic characterization of the anisotropic behaviour of air-saturated porous materials. Ultrasonics 1998;36:323–41.
[6] Tarnow V. Airflow resistivity of models of fibrous acoustic materials. J Acous Soc Am 1996;100:3706–13.
[7] Tarnow V. Calculation of the dynamic air flow resistivity of fiber materials. J Acous Soc Am 1997;102:1680–8.
[8] Tarnow V. Measurement of sound propagation in glass wool. J Acous Soc Am 1995;97:2272–81.
[9] Gibiat V, Laloe F. Acoustical impedance measurements by the two-microphone–three-calibration (T.M.T.C.) method. J Acous Soc Am 1990;88:2533–45.
[10] Castagnède B, Henry M, Leclaire P, Kelders L, Lauriks W. Acoustical characterization of fibrous materials and modelling with no adjustable parameter. C R Acad Sci Paris 1996;II 323:177–83.
[11] Allard JF, Henry M, Tizianel J. Sound propagation in air-saturated random packings of beads. J Acous Soc Am 1998;104:2004–7.